Biosensors and Bioelectronics 33 (2012) 228–232

Contents lists available at SciVerse ScienceDirect

Biosensors and Bioelectronics

journal homepage: www.elsevier.com/locate/bios

Triplex signal amplification for electrochemical DNA biosensing by coupling probe-gold nanoparticles–graphene modified electrode with enzyme functionalized carbon sphere as tracer

Haifeng Dong [a], Zhu Zhu [a], Huangxian Ju [a,*], Feng Yan [b,*]

[a] State Key Laboratory of Analytical Chemistry for Life Science, Department of Chemistry, Nanjing University, Nanjing 210093, PR China
[b] Jiangsu Institute of Cancer Prevention and Cure, Nanjing 210009, PR China

ARTICLE INFO

Article history:
Received 25 October 2011
Received in revised form 9 December 2011
Accepted 6 January 2012
Available online 16 January 2012

Keywords:
DNA biosensor
Electrochemical biosensing
Sequence analysis of DNA
Electrochemically reduced graphene
Signal amplification
Carbon sphere

ABSTRACT

An ultrasensitive electrochemical DNA biosensor was constructed by assembling probe labeled gold nanoparticles (ssDNA–AuNP) on electrochemically reduced graphene oxide (ERGO) modified electrode with thiol group tagged (GT) DNA strand ($d(GT)_{29}SH$) and coupling with horseradish peroxidase (HRP) functionalized carbon sphere (CNS) as tracer. The heteronanostructure formed on the biosensor surface appeared relatively good conductor for accelerating the electron transfer, while the HRP tagged CNS provided dual signal amplification for electrochemical biosensing. The triplex signal amplification strategy produced an ultrasensitive electrochemical detection of DNA down to attomolar level (5 aM) with a linear range of 5 orders of magnitude (from 1×10^{-17} M to 1×10^{-13} M), and appeared high selectivity to differentiate single-base mismatched and three-base mismatched sequences of DNA. The proposed approach provided a simple and reliable method for DNA detection with high sensitivity and specificity, indicating promising application in bioanalysis and biomedicine.

1. Introduction

The sensitive detection of DNA sequence has emerged as a hot subject of research due to its extensive applications in molecular diagnostics, food, environment, anti-terrorism and forensic science (Dong et al., 2008; Sassolas et al., 2008; Bi et al., 2010; Dong et al., 2010a). Although various approaches have been employed for detection of low-abundant DNA, such as polymerase-chain-reaction (PCR) technique (Ju et al., 2003; Ye et al., 2003), enzymatic cycles (Munge et al., 2005; Wang et al., 2008), and nanoparticles-based signal amplification (Taton et al., 2000; Song et al., 2009), novel detection technology or signal amplification strategies are continually needed to meet the increasing demands (Wang et al., 2008). Multiple signal amplification strategy opens new opportunities for highly sensitive detection of biomolecules (Li et al., 2010). For example, two dual signal amplification strategies have been developed for detection of DNA hybridization by combining the efficient carrier-bead amplification platform with sensitive stripping voltammetric measurement (Dong et al., 2010b) and carbon nanotubes carrier amplification approach with enzymatic cycle (Gao et al., 2011).

In electrochemical biosensing, the electrocatalytic properties are strongly related to the microstructure and surface chemistry of biosensors. Recently, graphene has been used for construction of biosensors due to its unique electronic properties and large accessible surface area (Stankovich et al., 2006; Li et al., 2008; Zhou et al., 2009). A novel electrochemical immunosensor with greatly enhanced sensitivity for detection of α-fetoprotein (AFP) based on graphene modified electrode has been developed (Du et al., 2010). Biocompatible graphene not only facilitates bimolecular binding but also accelerates electron transfer, thus amplifies electrochemical detection signal (Kang et al., 2009; Wang et al., 2009a). Furthermore, the graphene modified electrode displays a superior biosensing performance in comparison to carbon nanotubes modified electrode (Alwarappan et al., 2009).

This work used electrochemically reduced graphene oxide (ERGO) modified electrode to assemble probe labeled gold nanoparticles (ssDNA–AuNP) with thiol group-DNA strand ($d(GT)_{29}SH$) and develop a triplex signal amplification strategy for DNA detection by coupling with streptavidin (SA)–horseradish peroxidase (HRP) functionalized carbon sphere (CNS) as a signal tag. The ERGO modified electrode was prepared by electrochemical reduction of graphene oxide (GO) coated on a glassy carbon electrode (Guo et al., 2009). The $d(GT)_{29}SH$ was then assembled on the electrode by the π–π stacking interaction between $d(GT)_{29}$ and ERGO (Zheng et al., 2003) for anchoring ssDNA–AuNPs to

* Corresponding authors. Tel.: +86 25 83593593, fax: +86 25 83593593.
E-mail addresses: hxju@nju.edu.cn (H. Ju), yanfeng2007@sohu.com (F. Yan).

0956-5663/$ – see front matter © 2012 Elsevier B.V. All rights reserved.
doi:10.1016/j.bios.2012.01.006

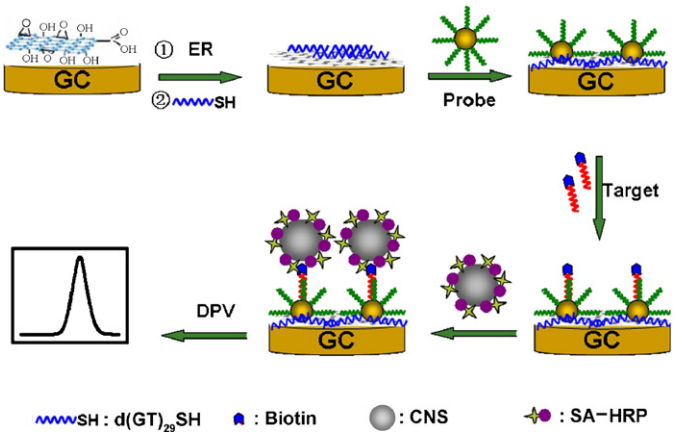

Fig. 1. Schematic presence of electrochemical DNA biosensing using probe labeled AuNPs–graphene modified electrode and enzyme functionalized carbon sphere for DPV tracing.

produce a DNA biosensor (Fig. 1). The heteronanostructure of the biosensor surface appeared high conductivity for accelerating the electron transfer (Liu et al., 2010). After hybridization of the immobilized DNA probe with biotinylated target, the signal tag was bound to the biosensor by the specific recognition of SA to biotin. An enzymatic reaction of HRP was finally used to produce detection signal. The proposed strategy showed high sensitivity and selectivity toward DNA detection, which provides a useful platform for bioanalytical and clinic biomedical application.

2. Materials and methods

2.1. Reagents

1-Ethyl-3-(3-dimethylaminopropyl) carbodiimide hydrochloride (EDC), *N*-hydroxysuccinimide (NHS), HRP labeled SA, tris-(2-carboxyethyl) phosphine hydrochloride (TCEP) and salmon DNA were purchased from Sigma–Aldrich, Inc. (USA). Tris(hydroxymethyl)aminomethane (tris)–HCl (10 mM, pH 8.0) containing 1 mM ethylenediaminetetraacetic acid (EDTA) (10 mM tris, 1 mM EDTA, 50 mM NaCl, 10 mM $MgCl_2$) was used as DNA hybridization buffer. 0.05% Tween-20 was spiked into phosphate buffered saline (PBS) as wash buffer (PBST) to minimize unspecific adsorption. DNA was stored in Tris–HCl (10 mM, pH 8.0) containing 1 mM EDTA. All other reagents were of analytical grade. All aqueous solutions were prepared using ultra-pure water (18 MΩ, Milli-Q, Millipore). The oligonucleotides were purchased from Sangon Biological Engineering Technology & Co. Ltd. (Shanghai, China) and purified using high-performance liquid chromatography. Their sequences were:

three-base mismatched oligonucleotide: 5′biotin-CCG A**T**G AGA C**G**T TTC C**C**T TCG AC3′;

single-base mismatched oligonucleotide: 5′biotin-CCG AAG AGA C**G**T TTC CGT TCG AC3′;

target: 5′biotin-CCG AAG AGA CCT TTC CGT TCG AC3′;

probe: 5′HS-C_6GT CGA ACG GAA AGG TCT CTT CGG3′;

$d(GT)_{29}SH$: 5′HS-C_6GTG TG TGT GTG TGT GTG TGT GTG TGT GT GTG TGT GTG TGT GTG TGT GTG TGT GTG TGT3′.

2.2. Apparatus

The morphology of CNS was examined with scanning electron micrograph with a Hitachi S-4800 (Japan). The morphologies of the ERGO and ssDNA–AuNPs loaded ERGO were recorded on a JEM 2100 transmission electron microscope (TEM). Fourier transform infrared spectra were recorded on a Nicolet 400 Fourier transform infrared spectrometer (Madison, WI). The dynamic light-scattering measurement (DLS) was recorded on 90 Plus/BI-MAS Brook haven (USA). Electrochemical experiments were performed on a CHI 630A Electrochemical Workstation (CH Instruments, USA) with a three-electrode system using Pt as counter electrode and saturated calomel electrode as reference electrode.

2.3. Electrochemical reduction of GO and preparation of DNA biosensor

The GO coated GCE was prepared by firstly polishing a GCE with alumina powders, then rinsing thoroughly and drying it with blowing N_2, and finally spreading 5 μL exfoliated GO suspension (6 mg/mL) on the GCE. The film was dried in a vacuum desiccator. The electrochemical reduction of the exfoliated GO film on GCE was carried out with cyclic voltammetric sweep between −1.5 and 0.1 V at 100 mV/s in 10 mM pH 5.0 PBS (K_2HPO_4/KH_2PO_4).

4.4 μL $d(GT)_{29}SH$ (2 μM) was dropped on the ERGO modified GCE, and reacted at room temperature for 3 h. After the GCE was washed thrice with PBST, 5 μL ssDNA–AuNPs (9.2 nM) was added to the GCE surface and incubated at room temperature for 12 h. It was then rinsed with PBST to remove the unbound ssDNA–AuNPs and blocked with 5 μL 1 mg/mL salmon DNA to reduce nonspecific adsorption for obtaining the DNA biosensor.

2.4. Preparation of ssDNA–AuNPs

The preparation of ssDNA–AuNPs was according to a previous report (Liu and Lu, 2006). Briefly, a disposable vial used for synthesis (20 mL volume) was dipped in 12 M NaOH for 1 h at room temperature and rinsed with copious amounts of deionized water. 9 μL of 0.1 mM thiol-modified DNA, 1 μL of 500 mM acetate buffer (pH 5.2) and 1.5 μL of 10 mM TCEP were mixed and incubated at room temperature for 1 h to activate the thiol-modified DNA. Then the activated DNA was added to vial containing 1.56 mL AuNPs (2.6 nM, diameter 13 nm) and reacted for 16 h at room temperature. 15.6 μL of 500 mM tris acetate (pH 8.2) buffer was then added to vial with gentle hand shaking. The resulting ssDNA–AuNPs was stored at 4 °C.

2.5. Assembly of SA–HRP tagged CNS

Colloidal CNS was synthesized from fructose in closed systems under hydrothermal conditions (Shin et al., 2008). The CNS was functionalized with hydrophilic carboxylate groups by sonication in 6:1 concentrated H_2SO_4/HNO_3 for 1 h (Sun and Li, 2004). The resulting CNS (0.5 mL) was mixed with 0.5 mL SA–HRP (3 mg/L) in the presence of EDC (20 mg/mL) and NHS (30 mg/mL), and incubated for 1 h at room temperature to obtain the SA–HRP tagged CNS.

2.6. DNA detection

The hybridization reaction was carried out by dropping 5 μL of the target solution to the biosensor and incubation at room temperature for 1 h. After the biosensor was washed thoroughly with PBST, 5 μL SA–HRP tagged CNS (0.5 mg/mL) was dropped on its surface, which was left for 30 min and washed PBST to remove the unbound SA–HRP tagged CNS. The different pulse voltammetric (DPV) measurements were performed from −300 to −850 mV with pulse amplitude of 50 mV and width of 50 ms. The data for condition optimization and the calibration curve were the average of three measurements.

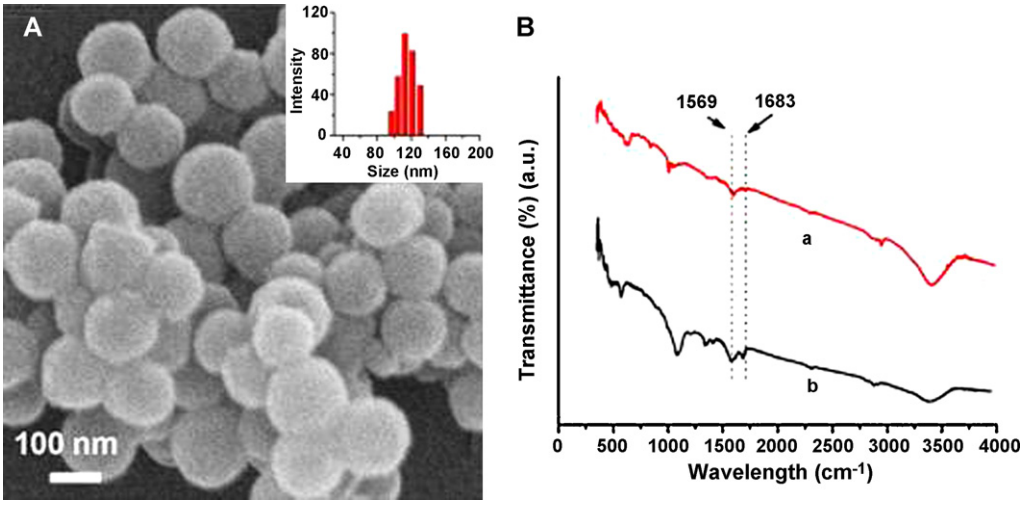

Fig. 2. (A) SEM of as-prepared CNS and (B) FT-IR spectra of CNS (a) and CNS–SA/HRP (b). Inset in A: DLS of prepared CNS.

3. Results and discussion

3.1. Characterization of CNS and SA–HRP tagged CNS

The CNS was obtained by a "green" synthetic approach, and functionalized with hydrophilic carboxylate groups by sonication in 6:1 concentrated H_2SO_4/HNO_3 for 1 h. The carboxylated CNS showed a homogeneous and smooth surface and good dispersion with a narrow size distribution (Fig. 2A). Their mean size was about 120 nm. The DLS further confirmed the narrow size distribution of the obtained CNS (inset in Fig. 2A). The hydrophilic surface could be easily functionalized with SA–HRP by covalent linking. In

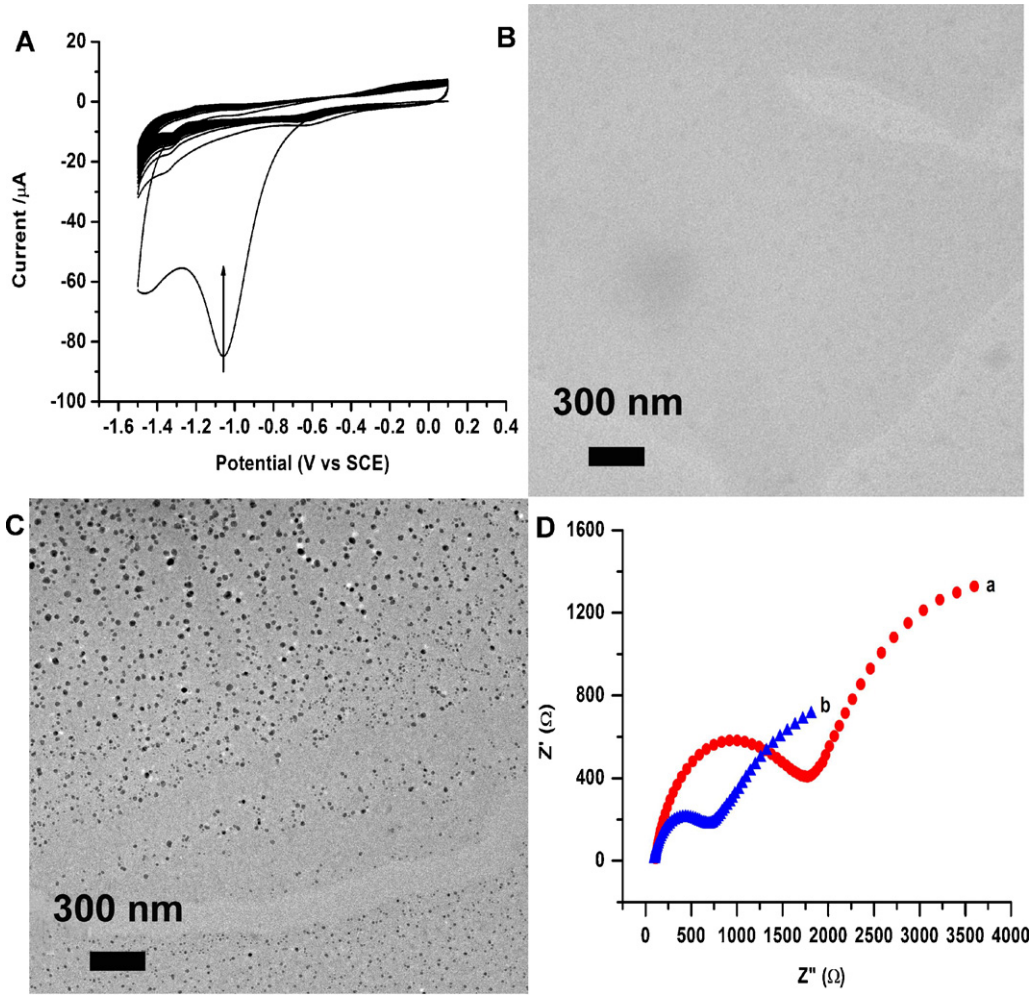

Fig. 3. (A) CV of GO modified GCE in nitrogen-saturated PBS (pH 5.2) at 50 mV/s, (B) TEM image of ERGO, (C) TEM image of ssDNA–AuNPs loaded ERGO, and (D) electrochemical impedance spectra of (a) GO and (b) ssDNA–AuNPs assembled ERGO modified GCEs in 0.1 M KCl containing 5 mM $K_3[Fe(CN)_6]$/$K_4[Fe(CN)_6]$.

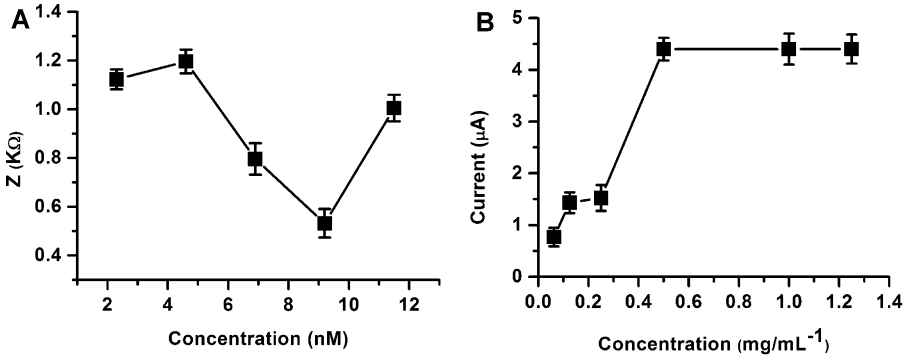

Fig. 4. (A) Electrochemical impedance at different concentrations of ssDNA–AuNPs and (B) plot of peak current *vs* HRP–CNS concentration.

comparison with the CNS (Fig. 2B, curve a), the Fourier transform infrared spectrum of the SA–HRP tagged CNS displayed obvious absorption peaks corresponding to the amide bands I (1683 cm^{-1}) and II (1569 cm^{-1}) of SA–HRP(Fig. 2B, curve b), respectively, indicating that the SA–HRP molecules were successfully loaded on the carboxylated CNS.

3.2. Characterization of electrode assembly process

The cyclic voltammogram (CV) of GO modified GCE showed a large reduction peak around −1.1 V, which was related to the reduction of the surface oxygen groups. The reduction current decreased considerably at the second cycle and disappeared after several potential scans (Fig. 3A). This phenomenon indicated that the reduction of surface-oxygenated groups on GO was quick and irreversible (Guo et al., 2009; Wang et al., 2009b; Shao et al., 2010). Transmission electron microscopic images showed few-layer flexible wrinkled sheet of ERGO (Fig. 3B). Benefiting from the strong π–π stacking between $d(GT)_{29}SH$ and ERGO, the ssDNA–AuNPs could be efficiently loaded on the surface of ERGO *via* Au—S bond (Fig. 3C). Furthermore, the colloidal AuNPs were distributed on the whole surface of ERGO sheets. It is worthy to mention that the direct assembly of DNA on heteronanostructure did not alter the structures and properties of both AuNPs and ERGO, including their high conductivity for accelerating the electron transfer. As shown in Fig. 3D, the GO modified GCE showed an electron-transfer resistance of about 2400 Ω, while ssDNA–AuNPs assembled ERGO modified GCE displayed a resistance of only about 800 Ω in spite of the presence of high content of ssDNA with negative charge of phospholipids, which would block the electron transfer of negatively charged $Fe(CN)^{3-/4-}$. The low resistance indicated the good conductivity of the ssDNA–AuNPs assembled ERGO.

3.3. Optimization of biosensing condition

The amount of ssDNA–AuNPs attached on the ERGO sheet and the concentration of the tracer affected intensely the electrochemical performance of the proposed sensor for detection DNA target (Fig. 4). The electron-transfer resistance decreased along with the increase of the Au–ssDNA concentration with the lowest value observed at 9.2 nM (Fig. 4A). The further increase of Au–ssDNA caused the increasing electron-transfer resistance, which might result from the citrate moieties on AuNPs (Gao et al., 2011). The electrochemical response was intensified in a tracer concentration-dependent manner, and tended to a stable value at 0.5 mg/mL (Fig. 4B). Thus, 9.2 nM ssDNA–AuNPs and 0.5 mg/mL SA–HRP–CNSs were used in all subsequent works, respectively.

3.4. Signal amplification

After the proposed biosensor hybridized with the biotinylated target and incubated with SA–HRP tagged CNS solution for 30 min, respectively, it exhibited a stable DPV peak at −0.564 V in PBS containing o-phenylenediamine and hydrogen peroxide, which corresponded to the reduction of 2,2′-diaminoazobenzene, the enzymatic product (Cheng et al., 2008). The tracer made each target hybridization event relate to numerous enzyme reaction, thus greatly amplify the detection signal. As a comparison, SA–HRP was used as the tracer instead of SA–HRP–CNS. As shown in Fig. 5, the signal originated from SA–HRP–CNS tracer (curve a) was 3.6-fold larger than that from SA–HRP (curve b) at 0.1 fM target DNA, and 6.8-fold larger than the background (curve c), which was detected in absence of target and came from the nonspecific adsorption of SA–HRP–CNS. This result demonstrated that the SA–HRP–CNS tracer greatly amplified the detection signal.

3.5. Voltammetric analysis of target DNA

Under optimal conditions, the DPV peak current increased with the increasing concentration of target DNA (Fig. 6A). The plot of the response *vs* the logarithm of target concentration showed a linear relationship in the detected range from 1×10^{-17} M to 1×10^{-13} M (inset in Fig. 6A). At the current signal of 3 times standard deviation (SD) measured at free of target DNA, the limit of detection (LOD) was calculated to be 5 aM. Compared to other enzyme-based electrochemical DNA sensors (Munge et al., 2005; Wang et al., 2008), the proposed biosensor showed a much lower limit of detection. The limit of detection was also competitive with other highly

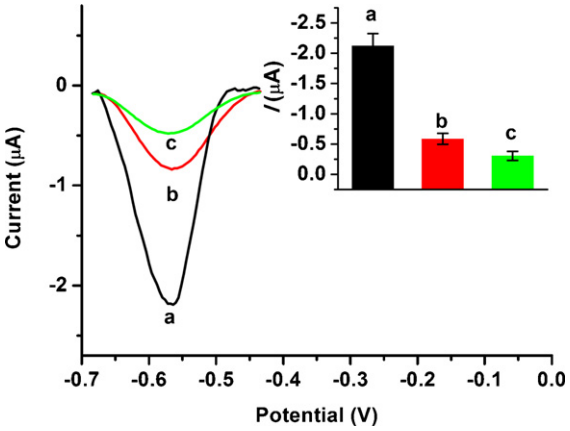

Fig. 5. DPV curves of (a) 0.1 fM target with SA–HRP–CNS tracer, (b) 0.1 fM target with SA–HRP tracer and (c) blank with SA–HRP–CNS tracer. Inset: the corresponding peak currents.

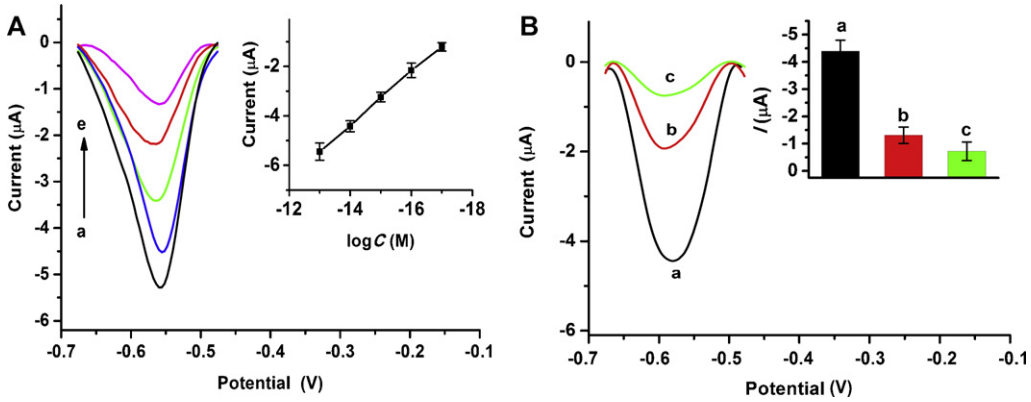

Fig. 6. (A) DPV curves at target DNA concentrations of 0.1, 0.01 pmol/L, 0.1, 0.01 fmol/L from (a) to (e) and (B) DPV curves at 0.01 pM complement sequence (a), single-base mismatched sequence (b) and three-base mismatched sequence (c). Inset in A: linear relationship between peak current and logarithm of target concentration ($n = 3$). Inset in B: the corresponding current values.

sensitive detection approaches such as molecular biological technique (Saghatelian et al., 2003; Tan et al., 2005; Mahmoudian et al., 2008), and nanoparticle-based signal amplification strategy (Liu et al., 2008; Pinijsuwan et al., 2008; Rijiravanich et al., 2008). The high sensitivity emphasized the importance of the proposed triplex signal amplification strategy to the improved analytical performance of the biosensor.

The specificity of the proposed DNA biosensor was investigated by exposing it to three kinds of DNA sequences, including perfect complementary target, single-base mismatched oligonucleotide and three-base of mismatched oligonucleotide at the same concentration (0.01 pM). The biosensor exhibited good performance to discriminate perfect complementary target and the base mismatched targets (Fig. 6B). The perfect complementary target showed a signal of 3.4-fold and 6.6-fold of those single-base mismatched oligonucleotide and three-base mismatched oligonucleotide, respectively, indicating good selectivity and great potential for single nucleotide polymorphism analysis.

4. Conclusions

This work has demonstrated a highly sensitive electrochemical DNA detection platform based on a triplex signal amplification strategy using probe labeled gold nanoparticles–graphene modified electrode and enzyme functionalized carbon sphere as tracer. The DNA mediated noncovalent assembly of AuNPs–graphene heteronanostructure does not alter the structures and properties of AuNPs and ERGO, which makes the ssDNA–AuNPs–ERGO maintain relatively good conductivity. The SA–HRP–CNS tracer enables the hybridization event relating to numerous enzyme reactions, providing dual signal amplification for ultrasensitive detection of DNA. This novel triplex signal amplification strategy can detect target DNA down to attomolar level with high selectivity to differentiate single-base mismatched and three-base mismatched sequences of DNA. The proposed approach would be attractive for genetic target analysis in bioanalytical and clinic biomedical application.

Acknowledgments

This work was funded by National Basic Research Program of China (2010CB732400), National Natural Science Foundation of China (20875044, 21075055 and 21135002) and the Program for Leading Medical Talents from Department of Health of Jiangsu Province.

References

Alwarappan, S., Erdem, A., Liu, C., Li, C.Z., 2009. J. Phys. Chem. C 113, 8853–8857.
Bi, S., Zhang, J.L., Zhang, S.S., 2010. Chem. Commun. 46, 5509–5511.
Cheng, W., Ding, L., Lei, J.P., Ding, S.J., Ju, H.X., 2008. Anal. Chem. 80, 3867–3872.
Dong, H.F., Gao, W.C., Yan, F., Ji, H.X., Ju, H.X., 2010a. Anal. Chem. 82, 5511–5517.
Dong, H.F., Yan, F., Ji, H.X., Wong, D.K.Y., Ju, H.X., 2010b. Adv. Funct. Mater. 20, 1173–1179.
Dong, X.C., Lau, C.M., Lohani, A., Mhaisalkar, S.G., Kasim, J., Shen, Z.X., Ho, X.N., Rogers, J.A., Li, L.J., 2008. Adv. Mater. 20, 2389–2393.
Du, D., Zou, Z.X., Shin, Y., Wang, J., Wu, H., Engelhard, M.H., Liu, J., Aksay, I.A., Lin, Y.H., 2010. Anal. Chem. 82, 2989–2995.
Gao, W.C., Dong, H.F., Lei, J.P., Ji, H.X., Ju, H.X., 2011. Chem. Commun. 47, 5220–5222.
Guo, H.L., Wang, X.F., Qian, Q.Y., Wang, F.B., Xia, X.H., 2009. ACS Nano 3, 2653–2659.
Ju, H.X., Ye, Y.K., Zhao, J.H., Zhu, Y.L., 2003. Anal. Biochem. 313, 255–261.
Kang, X.H., Wang, J., Kang, X.H., Wu, H., Aksay, I.A., Liu, J., Lin, Y.H., 2009. Biosens. Bioelectron. 25, 901–905.
Li, J.S., Deng, T., Chu, X., Yang, R.H., Jiang, J.H., Shen, G.L., Yu, R.Q., 2010. Anal. Chem. 82, 2811–2816.
Li, X.L., Wang, X.R., Zhang, L., Lee, S.W., Dai, H.J., 2008. Science 319, 1229–1232.
Liu, J.W., Lu, Y., 2006. Nat. Protoc. 1, 246–252.
Liu, J.B., Li, Y.L., Li, Y.M., Li, J.H., Deng, Z.X., 2010. J. Mater. Chem. 20, 900–906.
Liu, G., Wan, Y., Gau, V., Zhang, J., Wang, L.H., Song, S.P., Fan, C.H., 2008. J. Am. Chem. Soc. 130, 6820–6825.
Munge, B., Liu, G.D., Collins, G., Wang, J., 2005. Anal. Chem. 77, 4662–4666.
Mahmoudian, L., Kaji, N., Tokeshi, M., Nilsson, M., Baba, Y., 2008. Anal. Chem. 80, 2483–2490.
Pinijsuwan, S., Rijiravanich, P., Somasundrum, M., Surareungchai, W., 2008. Anal. Chem. 80, 6779–6784.
Rijiravanich, P., Somasundrum, M., Surareungchai, W., 2008. Anal. Chem. 80, 3904–3909.
Saghatelian, A., Guckian, K.M., Thayer, D.A., Ghadiri, M.R., 2003. J. Am. Chem. Soc. 125, 344–345.
Sassolas, A., Leca-Bouvier, B.D., Blum, L.J., 2008. Chem. Rev. 108, 109–139.
Shao, Y.Y., Wang, J., Engelhard, M., Wang, C.M., Lin, Y.H., 2010. J. Mater. Chem. 20, 743–748.
Shin, Y.S., Wang, L.Q., Bae, I.T., Arey, B.W., Exarhos, G.J., 2008. J. Phys. Chem. C 112, 14236–14240.
Song, S.P., Liang, Z.Q., Zhang, J., Wang, L.H., Li, G.X., Fan, C.H., 2009. Angew. Chem. Int. Ed. 48, 8670–8867.
Sun, X., Li, Y., 2004. Angew. Chem. Int. Ed. 43, 597–601.
Stankovich, S., Dikin, D.A., Dommett, G.H.B., Kohlhaas, K.M., Zimney, E.J., Stach, E.A., Piner, R.D., Nguyen, S.T., Ruoff, R.S., 2006. Nature 442, 282–286.
Tan, E., Nguyen, J., Wong, D., Zhang, Y., Erwin, B., Ness, L.K.V., Baker, S.M., Galas, D.J., Niemz, A., 2005. Anal. Chem. 77, 7984–7992.
Taton, T.A., Mirkin, C.A., Letsinger, R.L., 2000. Science 289, 1757–1760.
Wang, Y., Lu, J., Tang, L.H., Chang, H.X., Li, J.H., 2009a. Anal. Chem. 81, 9710–9715.
Wang, J.X., Zhu, X., Tu, Q.Y., Guo, Q., Zarui, C.S., Momand, J., Sun, X.Z., Zhou, F.M., 2008. Anal. Chem. 80, 769–774.
Wang, Z.J., Zhou, X.Z., Zhang, J., Boey, F., Zhang, H., 2009b. J. Phys. Chem. C 113, 14071–14075.
Ye, Y.K., Zhao, J.H., Yan, F., Zhu, Y.L., Ju, H.X., 2003. Biosens. Bioelectron. 18, 1501–1508.
Zheng, M., Jagota, A., Semke, E.D., Diner, B.A., Mclean, R.S., Lustig, S.R., Richardson, R.E., Tassi, N.G., 2003. Nat. Mater. 33, 8–342.
Zhou, M., Zhai, Y.M., Dong, S.J., 2009. Anal. Chem. 81, 5603–5613.